The Egyptian Journal of Radiology and Nuclear Medicine (2014) **45**, 859–867

Egyptian Society of Radiology and Nuclear Medicine

The Egyptian Journal of Radiology and Nuclear Medicine

www.elsevier.com/locate/ejrnm
www.sciencedirect.com

ORIGINAL ARTICLE

MR spectroscopy and diffusion MR imaging in characterization of common sellar and supra-sellar neoplastic lesions

Faten Fawzy Mohammad [a,*], **Doaa Ibrahim Hasan** [a], **Mohamed Gouda Ammar** [b]

[a] *Diagnostic Radiology Department, Zagazig University, Egypt*
[b] *Neurosurgery Department, Zagazig University, Egypt*

Received 18 February 2014; accepted 11 April 2014
Available online 5 May 2014

KEYWORDS

MRS;
DWI;
Supra-sellar

Abstract *Background:* MR spectroscopy and diffusion-weighted imaging are useful non invasive imaging modalities used for characterization of different sellar and suprasellar lesions.
Patient and methods: We studied 30 cases of suprasellar SOLs (as proved by conventional MRI), MRS and DWI. Our findings were correlated with histopathological analysis after surgical resection.
Results: Three false positive cases in which cMRI give diagnosis mismatched with that obtained after adding the MRS findings and ADC values. MR spectrum type IIC is found in macroadenoma, craniopharyngioma, meningioma and germinoma with characteristic broad lipid peak in the second and forth types and elevated alanine peak in meningioma. Glioma had MRS appearance of type IIB. Simple differentiation between tumor types were achieved by the mean ADC values which were statistically significant ($p < 0.001$) when correlated to the histological diagnosis. When the ADC value of 0.6×10^{-3} mm^2/s this strongly points to macroadenoma, ADC value of 1.05×10^{-3} mm^2/s in meningiomas, ADC value $1.88\,8 \times 10^{-3}$ mm^2/s strongly points to craniopharyngioma, while gliomas and germinoma had ADC values 1.6×10^{-3} mm^2/s and 1.0×10^{-3} mm^2/s respectively.
Conclusion: MR spectroscopy and DWMRI are considered important diagnostic tools complementary to cMRI in pre-surgical evaluation and discrimination between different sellar and suprasellar lesions.

1. Introduction

Accurate diagnosis is essential for optimum clinical management of patients with sellar and supra-sellar tumors. Currently, there is a widespread use of MRI in determining tumor extent for surgery and radiotherapy planning as well as for post therapy monitoring (1–3).

* Corresponding author. Tel.: +20 1224444297.
E-mail addresses: Fatenfawzy25@hotmail.com (F.F. Mohammad), dididodge@yahoo.com (D.I. Hasan), ammarmg@gmail.com (M.G. Ammar).
Peer review under responsibility of Egyptian Society of Radiology and Nuclear Medicine.

0378-603X © 2014 Production and hosting by Elsevier B.V. on behalf of Egyptian Society of Radiology and Nuclear Medicine.
Open access under CC BY-NC-ND license. http://dx.doi.org/10.1016/j.ejrnm.2014.04.012

Pituitary tumors are classified into tumors of adenohypophyseal cells (adenoma and carcinoma) and other pituitary tumors of the sellar region that include; craniopharyngioma, schwannomas, germ cell tumors, neuronal tumors (ganglioneuromas), mesenchymal tumors, gliomas, chordomas and metastatic tumors (4).

Recently, diffusion-weighted magnetic resonance imaging (DWI) has been used in the investigation of intracranial tumors (5–7). DW imaging allows the measurement of tissue water diffusion, which is affected by the size and integrity of structures that normally restrict diffusion, in the brain. The apparent diffusion coefficient (ADC) can be increased as a result of pathologic processes that modify tissue integrity, and thus these processes reduce "restricting" barriers (8).

At present ^{1}H-MRS represents a standard method for clinical evaluation of intracranial tumors (9,10). It provides noninvasively a wide spectrum of the biochemical information, which can be used for differentiation of neoplastic and non-neoplastic pathology, estimation of the tumor type, grade and proliferative activity, prediction of the response to therapy and prognosis, and monitoring of the therapeutic response. The majority of published ^{1}H-MRS studies are devoted to investigation of parenchymal brain lesions, whereas only few reports dealt with supra-sellar neoplasm. The reason for this is evident—in such cases it is difficult to get good quality spectra, because clinical MR imagers with magnetic field strength of 1.5 Tesla usually do not permit to use ^{1}H-MRS voxel, less than 1 cc, which results in its frequent contamination with skull base structures (11,12).

2. Patients and methods

The study was carried in the time frame between June 2012 and September 2013, included 30 consecutive patients referred from Neurology and Neurosurgery Departments to the MR unit, Radiology Department, Zagazig University. All our patients were known cases of sellar and/or supra-sellar SOL as proved by CT and MRI. The study was approved by the local ethics committee and informed consent was obtained from the patients.

2.1. Imaging sequences

(1) cMRI with a 1.5 T clinical imager (Philips Medical System-Achiva-class II, USA) equipped with a standard head coil. The following protocol was used:
   - Non contrast axial, coronal and sagittal T1WIs (TR 400–550 m/s, TE 15 m/s, FOV 250, matrix 256 × 256, section thickness 3 mm, interslice gap 1 mm).
   - Axial T2WI (TR 3500–4800 m/s, TE 110 m/s, FOV 250, matrix 256 × 256, slice thickness 3 mm, interslice gap 1 mm).
   - Post contrast coronal and sagittal T1WI after administration of gadolinium 0.1 mm/kg body weight.

(2) Prior to contrast agent administration, breath hold DWI was done with a single-shot spin-echo echo-planner sequence (TR/TE: 2000/33–55, matrix size 128 × 128, section thickness 6 mm, interslice gap 1 mm, FOV 38 cm, *b* values 0 and 1000 s/mm^2).

(3) ADC maps were calculated automatically and ADC values were measured by using circumferential ROI (8–50 mm^2) in the central and solid appearing portions of lesions.

(4) Single voxel MRS was performed by applying the voxel on the region of the interest which was the solid part of the lesion. Single voxel acquisition was used and data from the voxel were obtained using a point resolved spectroscopy sequence (TR 2000 m/s, TE 135 m/s).

The time domain signal intensity was recognized and processed to remove residual water signal. Post processing of the spectroscopic data consisted of frequency shift and phase and linear baseline corrections after Fourier transformation. Frequency domain curve was fitted by the manufacturer to define metabolites. The main metabolites identified by ^{1}H-MRS were NAA at 2.0 ppm, Cr at 3.0 ppm, Cho-containing compounds at 3.2 ppm, myoinositol (mI), lactate as a doublet at 1.33 ppm and lipids resonating between 0.8 and 1.4 ppm. Presence of each metabolite peak was initially evaluated qualitatively by visual inspection, and type of the pathological ^{1}H-MR spectra was determined according to the previously proposed classification (Table 1). Type I if NAA is the predominant peak, type II if the Cho is the predominant peak and type III if the predominant peak is not NAA or Cho. Each type further sub-typing into A, B ad C according to specific spectral findings e.g. in types I and II if there is Lip peak, it is given the subtype C. If No Lip peak it is given A or B (according to Lac peak). Type III is subdivided differently, if the predominant peak in the spectrum is Lipid, it is given the subtype A, or B (according to Cho peak). Type IIIC (the flat spectrum), if the MRS does not detect metabolite peaks at all (13,14).

2.2. Operative data

Operative approach was guided according to preoperative diffusion MRI and MRI spectroscopy. All pituitary adenomas operated by endoscopic trans-septal trans sphenoidal approach where curettage and suction could remove most of the midline tumor and different angles rigid endoscope enabled surgeons for better visualization and inspection of sellar and parasellar contents.

- Good evaluation of sphenoid sinus anatomy, defining sinus type (conchal, presellar, sellar), and sinus septa whether midline or paramedian.
- Sellar localization was confirmed intra-operatively by the C-arm.
- Other sellar lesions which may need proximal vascular control as meningioma, glioma, craniopharyngioma, teratoma, dermoid operated by microscopic subfrontal approach and frontal craniotomy.
- All patients kept at least one night at ICU for the assessment of postoperative courses regarding conscious level, visual, clinical, the fluid chart, electrolytes disturbances and managing complications if any.

2.3. Histopathological diagnosis

Our diagnosis was confirmed pathologically after surgical treatment.

Table 1 Determination of the type of pathological ^{1}H-MRS (14,15).

Type of the pathological ^{1}H-MR spectra	Predominant peak	Lac peak	Lip peaks
IA	NAA	No	No
IB	NAA	Yes	No
IC (with mild elevation of Lip)	NAA	–	Yes
IC (with moderate elevation of Lip)	NAA	–	Yes
IIA	Cho	No	No
IIB	Cho	Yes	No
IIC (with mild elevation of Lip)	Cho	–	Yes
IIC (with moderate elevation of Lip)	Cho	–	Yes
IIIA	Lip (Cho peak preserved)	–	Yes
IIIB	Lip (reduced or absent Cho peak)	–	Yes
IIIC	Absent any detectable metabolite peak		

2.4. Data analysis

Data analysis was performed using the SPSS (v15) statistical software package. ADC values were expressed as mean ± SD. Using ANOVA test as analytic tool for comparison of mean ADC values among different histological diagnosis (p value $\leqslant 0.001$, considered significant).

3. Results

This study included 30 patients with suprasellar lesions as diagnosed on cMRI. They were 18 females (60%) and 12 males (40%) and their age distribution ranged from 9 years to 55 years with a mean age of 24.6 ± 12.9 years. The most common age group was 20 to < 30 years (10 patients). All our cases were evaluated clinically. The most frequent clinical presentation was headache with visual disturbance as detected in 19/30 (63.3%) patients (Table 2).

According to imaging findings based on cMRI, MRS and ADC different pathological entities were detected (Table 3).

On MRS, macroadenoma is characterized by a significant reduction in NAA, moderate elevation of Cho, reduced Cr and frequent small Lip/Lac peaks. Seven tumors had type IIC, two cases showed type IIIB, two cases showed type IIIC and two cases had type IA. By diffusion MRI, 9 cases displayed hyperintense signal on DWI which is consistent with restricted diffusion, while 4 cases displayed hypointense signal of unrestricted diffusion, the mean ADC value in the 9 cases was 0.68 ± 0.36 (mean ± SD), compared to the normal gray matter of the adjacent temporal lobe (Fig. 1).

Five cases were diagnosed as craniopharyngiomas on cMRI depending on characteristic MR imaging features. On MRS, 3 cases showed type IIC spectrum with a broad Lip peak (Fig. 2). One case showed significant decrease of all metabolites, displayed type IIIC spectrum, while the last case revealed prominent choline peak, mild lactate with no detected lip peak (type IIB). Heterogeneous hypointense signal on DWI and hyperintense signal on the ADC map (Fig. 2). The mean ADC value was 1.91 ± 0.2 (mean ± SD) $\times 10^{-3}$ mm^2/s in 4 cases while the last case that displayed type IIB MR spectrum had a lower ADC value (1.4 ± 0.15 $\times 10^{-3}$ mm^2/s) and was proved pathologically to be of glial origin after surgical removal (Table 3).

Regarding the diagnosed cases of glial origin tumor; one of them was operated and underwent radiotherapy. The primary diagnosed cases showed type IIB spectrum with the prominent metabolite peak being Cho (Fig. 3), however the operated case showed no Cho peak but there is prominent lip peak which could be attributed to radiotherapy changes. The glial suprasellar tumors displayed heterogeneous signal on DWI and had ADC values of 1.57 ± 0.15 (mean ± SD) $\times 10^{-3}$ mm^2/s (Fig. 3).

Five cases of meningioma were diagnosed on c MRI, but on MRS, the diagnosis was confirmed in 2 cases that showed type IIC spectrum with an elevated Alanine peak (at 1.49 ppm), one case showed type IIIB, which is the case of recurrent meningioma under radiotherapy in a patient with neurofibromatosis type II while 2 cases revealed characteristic type IIC with no alanine peak.

The mean ADC value in 3 cases of meningiomas was 1.075 ± 0.17 (mean ± SD) $\times 10^{-3}$ mm^2/s with no diffusion restriction on DWI which is consistent with typical types, but the 2 cases with no alanine peak revealed restricted diffusion pattern with ADC value of 0.7 ± 36, this explained false positive diagnosis of meningioma on cMRI as they were diagnosed as macroadenomas and confirmed histopathologically (Table 3).

Table 2 Main clinical presentations in the 30 studied cases.

Clinical presentation	No. of patients (%)
Headache with visual disturbances	19(63.3%)
Headache with recurrent resistant vomiting	6(20%)
Isolated bilateral visual disturbance	2(6.6%)
Gigantism	1(3.3%)
Acromegaly	2(6.6%)

Table 3 Pathological types of the 30 cases based on cMRI, MRS and ADC.

The lesion	Based on cMRI no. of patients %	Based on MRS and ADC no. of patients %
Pituitary macroadenoma	13(43.3%)	15(50%)
Craniopharyngioma	5(16.6%)	4(13.3%)
Glioma	4(13.3%)	5(16.6%)
Meningioma	5(16.6%)	3(10%)
Germinoma	3(10%)	3(10%)

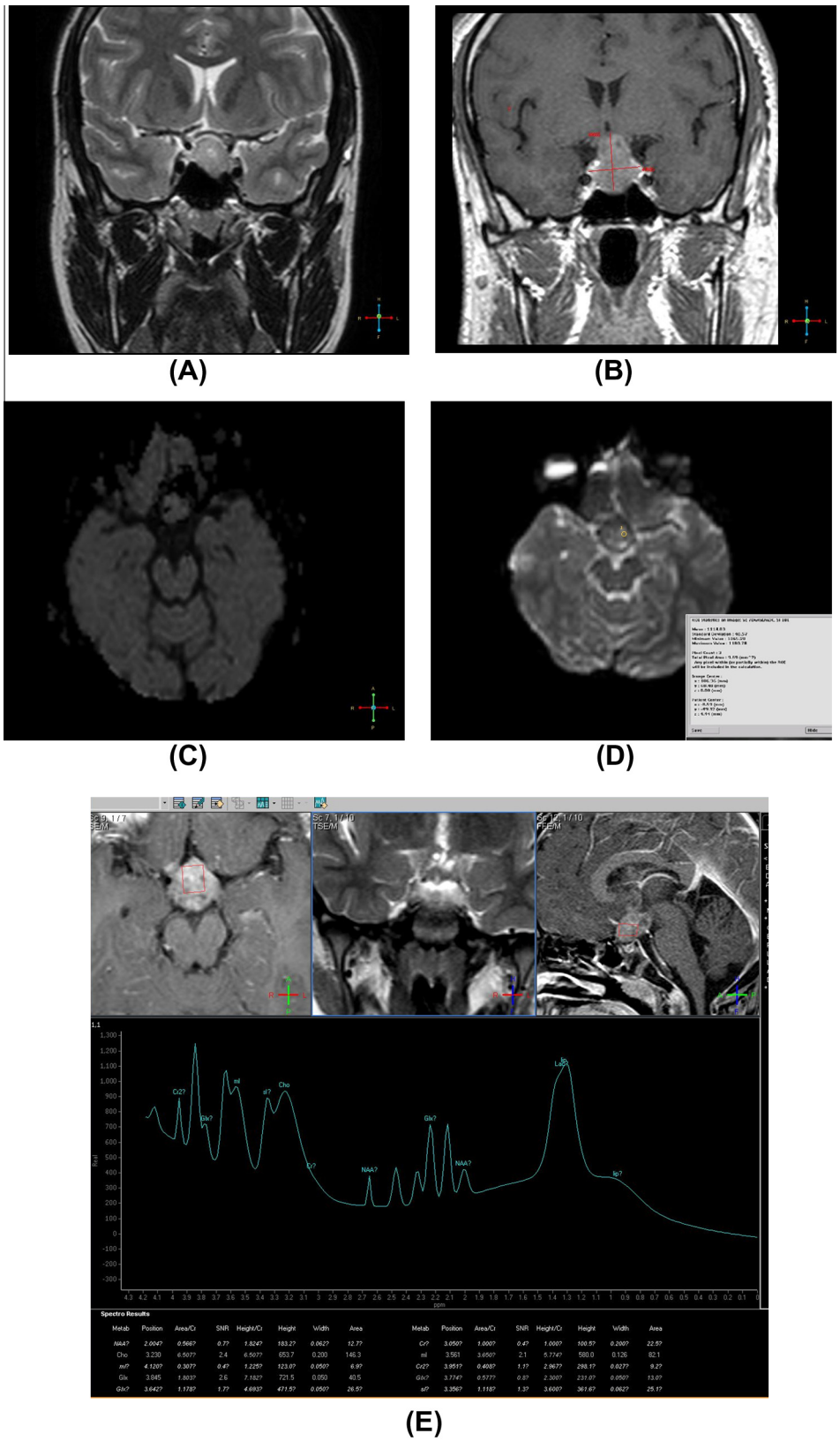

Fig. 1 A case of macroadenoma. 55-Year-old female patient presented with persistent headache. (A) Coronal T2WI revealed relatively hyperintense sellar SOL with supra-sellar and left para-sellar extension. (B) Coronal post Gd DTPA revealed homogeneous enhancement of the lesion. (C) Axial DWI revealed intermediate signal intensity of the lesion. (D) Axial ADC map revealed intermediate signal intensity of the lesion with ADC value = 1.1 denoting tumor with low cellularity (firm adenoma). (E) Single voxel MRS revealed type IIB: predominant Cho, reduced NAA, and mild Lip peak.

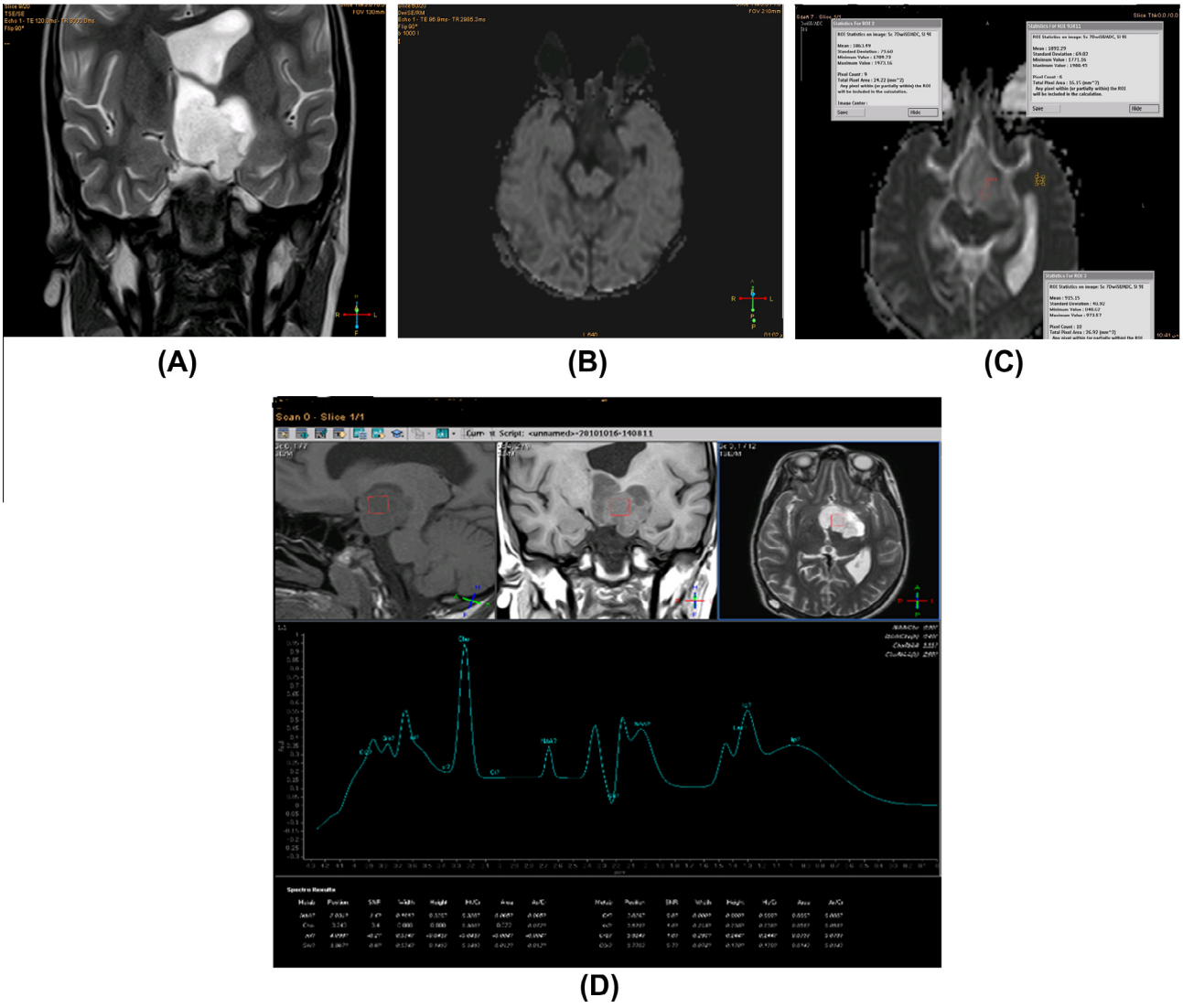

Fig. 2 A case of craniopharyngioma. 9-Year-old female presented with severe persistent headache. (A) Axial T2WI showing abnormal signal intensity lobulated lesion at the sellar and suprasellar region displays heterogeneous hyperintense signal. (B) Axial DWI showed heterogeneous hypointense supra-sellar lesion. (C) Axial ADC maps displayed heterogeneous hyperintensity of the lesion with ADC value = 1.7×10^{-3} mm^2/s. (D) Single voxel MRS revealed type IIC spectrum of the lesion by showing predominant peak of Cho, reduced NAA and broad Lip peak.

The three germinoma cases showed characteristic elevation of Cho, decreased NAA and Cr, along with prominent Lip peak type IIC. In DWI, the lesions displayed a hyperintense signal on DWI and intermediate signal intensity on the ADC map and had mean an ADC value of 1×10^{-3} mm^2/s (Fig. 4).

Using ANOVA as a statistical analytic tool = 27.5 $p < 0.001$. ADC values can significantly be correlated to the histological diagnosis ($p < 0.001$), for example, If the ADC value is 1.88×10^{-3} mm^2/s this strongly points to craniopharyngioma, but with the ADC value of 0.6×10^{-3} mm^2/s this strongly points to macroadenoma (Table 4).

4. Discussion

MRI can provide an initial diagnosis of an intracranial mass with a success rate of 30–90% (15). Proton MR Spectroscopy has been categorized as a safe diagnostic technique that can improve the non-invasive categorization of brain disorders and that they are starting to have a role in everyday clinical medicine (16).

In the present study we used long TE in MRS imaging as it allows good differentiation between lactate, lipid and alanine and lower base line distortion, similarly Mikhail et al. (17) and Majos et al. (18) used long TE. On the other hand, Fan et al. (11) used a short echo time in his study for brain gliomas and metastasis. Added that, metabolites such as myoinositol, are readily observed at short echo time only.

In our study we used single voxel MRS technique. Single voxel is considered to have major advantages when spatial resolution is not required. The advantages include short time requirement, quicker data processing for obtaining quantitative assessment and better magnetic field homogeneity (11,17). On the other hand Haughton et al. (16), recommended

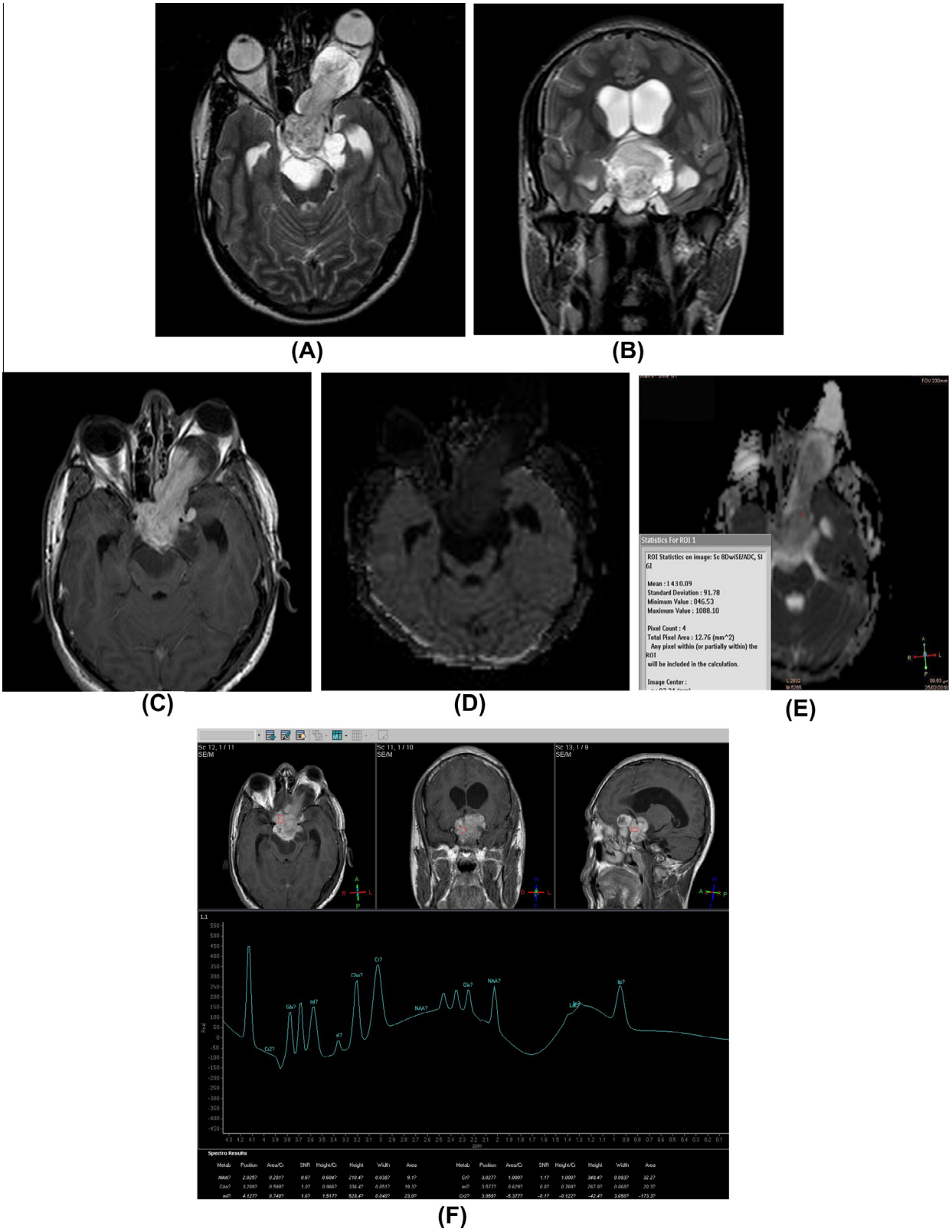

Fig. 3 A case of optic chiasma glioma. 17-Year old male patient presented with headache, vomiting, and bilateral diminution of vision and left sided proptosis. (A and B) Axial and coronal T2WI displayed hyperintense supra-sellar lesion with extension through the left optic foramen into the optic nerve with subsequent proptosis. (C) Axial T1WI post Gd DTPA revealed intense uniform enhancement of the lesion. (D) Axial DWI revealed hypointensity of the lesion, but relatively hyperintense to CSF excluding cystic lesion and support solid lesion with low cellularity. (E) Axial ADC map revealed inhomogeneous hyperintensity of the lesion with ADC value $= 1.4 \times 10^{-3}$ mm^2/s. (F) Single voxel MRS revealed type IIC spectrum: elevated Cho reduced NAA and mild Lip peak.

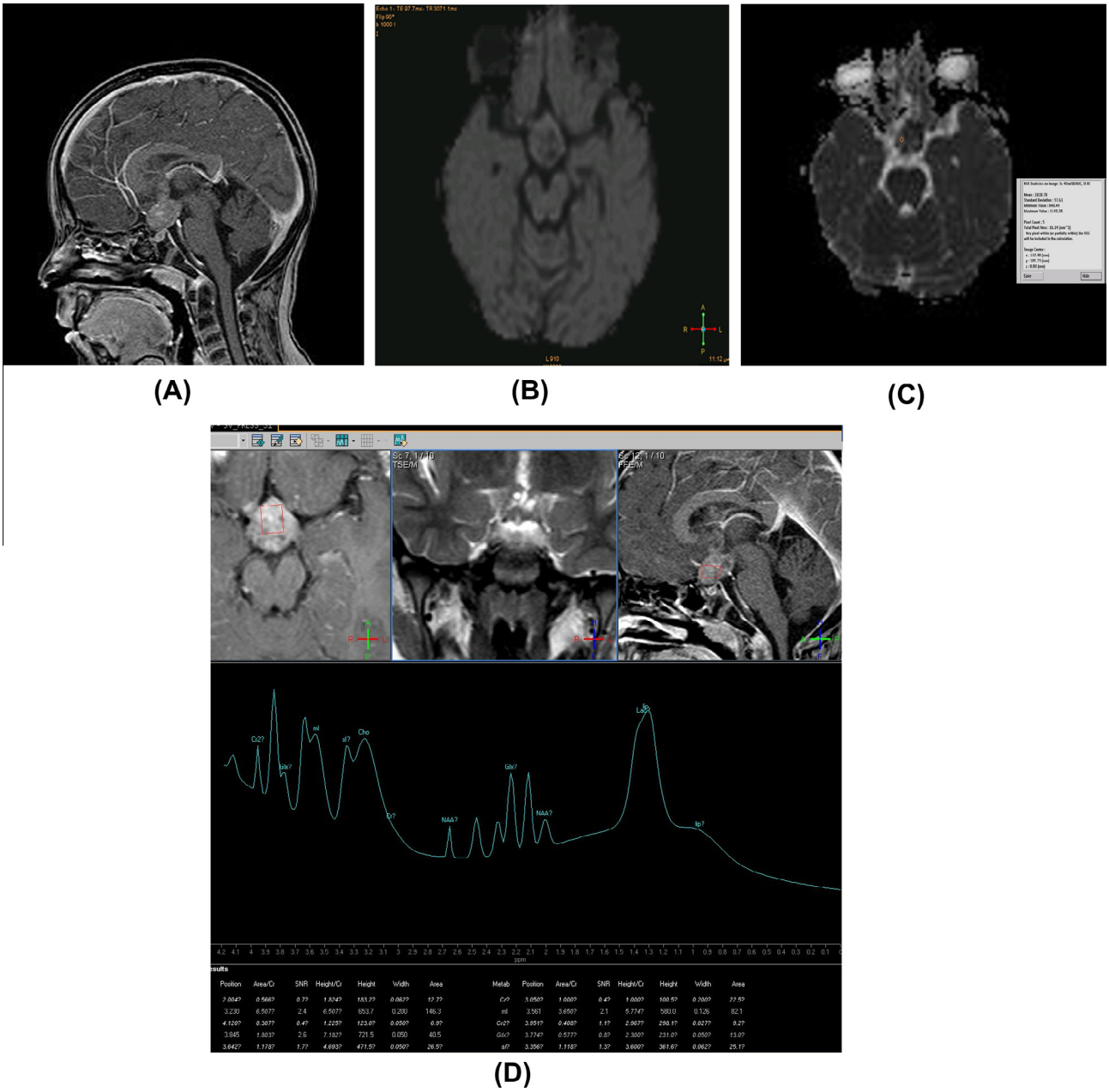

Fig. 4 A case of supra-sellar germinoma. 5-Year old female patient presented with bilateral diminution of vision. (A) Sagittal T1WI with Gd DTPA revealed supra-sellar SOL with mild inhomogeneous enhancement. (B) Axial DWI revealed slight hyperintense signal. (C) Axial ADC map showed intermediate signal intensity of the lesion with ADC value = 1.0×10^{-3} mm^2/s. (D) Single voxel MRS revealed type IIIA spectrum: predominant peak of Lip, high choline peak, and decreased NAA and only residual Cr.

Table 4 Showing comparison of mean ADC values among different histological diagnosis.

	No.	$X^- \pm$ SD (range)	Median
Macroadenoma	15	0.7 ± 0.28 (0.37–1.3)	0.6
Craniopharyngioma	4	1.9 ± 0.2 (1.7–2.2)	1.88
Glioma	5	1.57 ± 0.15 (0.4–1.7)	1.6
Meningioma	3	1.07 ± 0.17 (0.9–1.3)	1.05
Germinoma	3	1.0 ± 0.1(0.9–1.1)	1.00

multivoxel spectroscopy i.e. has higher SNR. In addition mutivoxel can provide information on tumor heterogeneity and infiltration not available by single voxel spectroscopy.

The most common suprasellar tumor in our study was the macroadenoma which revealed type IIC MRS metabolite profile pattern was in agreement with previous studies of Falini et al. (9), who stated that adenomas had pathological ^{1}H-MRS type IIC which was characterized by a significant reduction of the NAA peak, residual Cr peak, moderate elevation of Cho and infrequent presence of small Lip and Lac peaks. In our study all adenomas with type II were exclusively type IIC.

Regarding DWI we found a heterogeneous signal and different values for ADC according to their consistency. Nine cases displayed hyperintense signal on DWI which is consistent with restricted diffusion and had a mean ADC value of 0.68 ± 0.36 (mean ± SD), while 4 cases displayed hypointense signal of unrestricted diffusion with higher ADC values due to low cellularity. Our results were similar to Pierallini et al. (19) who stated that macroadenomas are of soft consistency with ADC values $(0.66 \pm 0.1) \times 10^{-3}$ mm^2/s, intermediate consistency with ADC values $(0.84 \pm 0.08) \times 10^{-3}$ mm^2/s and hard consistency with ADC values $(1.36 \pm 0.26) \times 10^{-3}$ mm^2/s. Moreover, Rogg et al. (20) stated in their studies that the DW signal and ADC values probably depend on the phase of hemorrhage and/or infarction in the pituitary gland or the pituitary adenoma.

In craniopharyngiomas cases we found MR spectra type IIC in three cases and III C in one case with a significant decrease of all metabolites, but we did not investigate any cysts. We focused the voxel over the solid portions of the tumor avoiding any cystic components. While Mikhail et al. (17) proved that 80% of craniopharyngioma showed type IIIC spectrum. He added that it seems that such a metabolic pattern resulted from the presence of calcifications and microcysts within the investigated volume of tissue. Elevated lipid peak with only small quantities of other metabolites correlated with the histological findings revealing high amounts of cholesterol in the cyst fluid.

Additionally craniopharyngiomas appeared as heterogeneously hypointense on DWI with high ADC values. In the current study, average ADC values for craniopharyngiomas was $(1.91 \pm 0.2) \times 10^{-3}$ mm^2/s. in agreement with Sener et al. (21).

MR spectra for our glioma cases were typically characterized by decreased NAA, Cr peaks and increase of Cho peak. Three tumors had pathological ^{1}H-MR spectra type II: 1 – type IIA, 2 – type IIB, and 3 – type IIC. The recurrent tumor showed type IIIB spectrum. In agreement with Mikhail et al. (17), but in disagreement regarding the spectrum of the recurrent glioma that showed type IIIC. Hypointense signal of low grade pilocytic astrocytoma is useful in the differential diagnosis because MR spectroscopy shows a high Cho level, low NAA and Lac peak despite the benign histology of the tumor (16).

On DWI, all of them showed hypointensity on DWI and hyperintensity on ADC map with mean ADC $(1.57 \pm 0.15) \times 10^{-3}$ mm^2/s which is consistent with low tumeral cellularity in consistence with Murakami et al. (22) who found that ADC values in pilocytic astrocytoma is often higher than 1.5×10^{-3} mm^2/s. High ADC value probably reflects relatively lower cellularity, a lower nuclear-to-cytoplasmic ratio and a high concentration of glycosaminoglycans, which is highly hydrophilic causing the shift of water molecules in the extracellular matrix.

Two meningioma cases in our study showed type IIC spectrum and an elevated alanine peak (at 1.49 ppm). These findings were partially consistent with those of Majos et al. (18) who stated that alanine is the most characteristic metabolite of meningioma, thus he considered it as a marker for meningioma. One case of meningioma showed type IIIB which was a recurrence under radiotherapy in a patient with neurofibromatosis type II. This is in agreement with Sumer (23) who also stated that post radiation lesions show a large peak between 0 and 2 ppm, indicating cell necrosis products.

Regarding the DWI of the meningioma cases appeared slightly hypointense in 3 out of 5 cases with an average ADC value of $1.07 \pm 17 \times 10^{-3}$ mm^2/s, while two cases with no alanine peak on MRS showed restricted diffusion with a mean ADC $(0.7 \pm 36 \times 10^{-3}$ mm^2/s,), so the diagnosis as meningioma on cMRI was incorrect and they were diagnosed as macroadenoma on MRS and DWI. Our results near the results reported by Okamoto et al. (24) in their study as they found that 66% of meningiomas (8 out of 12 cases) appeared isointense on DWI while partial hyperintensity was noted in the other cases (33%), while other authors found that the signal characteristics of meningiomas on DWI are variable (20).

Regarding germinoma cases in our study, typically characterized type IIC with moderate elevation of Lip, which was characterized by the absence of NAA peak, residual Cr peak, and significant elevation of Cho. This is in agreement with the authors (17). On DWI, we found them hyperintense on DWI (b1000) with an ADC value of $0.9–1.0 \times 10^{-3}$ mm^2/s. On the contrary Annette et al. (25) found that the majority of germinoma cases were isointense (54.4%) on DWI with normal diffusion and an ADC value of $0.94 \pm 0.54 \times 10^{-3}$ mm^2/s, while 36% were hyperintense on DWI with restricted diffusion and a mean ADC value of $0.69 \pm 0.74 \times 10^{-3}$ mm^2/s. They also found no significant correlation between the histological components and the ADC values.

In the current study, MRS and diffusion-weighted imaging are proved to be helpful as a non-invasive modality for the diagnosis of supra-sellar lesions. ADC values were statistically significant when correlated to the histological diagnosis ($p < 0.001$).

5. Conclusion

MRS and diffusion-weighted MRI are considered important diagnostic tools complementary to cMRI examination and promise to contribute to pre-surgical evaluation and discrimination between different suprasellar lesions.

Conflict of interest

None declared.

References

(1) Rennert J, Doerfler A. Imaging of sellar and parsellar lesions. Clin Neurol Neurosurg 2007;109:111–2.
(2) Dowling C, Bollen AW, Noworolski SM. Preoperative proton MR spectroscopic imaging of brain tumours: correlation with histopathologic analysis of resection specimens. Am J Neuroradiol 2001;22:604–12.
(3) Kwock L, Smith JK, Castillo M, Ewend MG, Cush S, Hensing T, et al. Clinical applications of proton MR spectroscopy in oncology. Technol Cancer Res Treat 2002;1:17–28.
(4) Sylvia L. Asa. Neuroendocrinology of hypothalamus and pituitary, Chapter 3. www.endotext.org/neuroend/index.htm [last updated 10.07.07].
(5) Brunberg J, Chenevert T, McKeever P, Ross D, Junck L, Muraszko K, et al. In vivo MR determination of water diffusion

coefficients and diffusion anisotropy: correlation with structural alteration in gliomas of the cerebral hemispheres. AJNR 1995;16:361–71.
(6) Byun W, Kim O, Kim D. MR imaging findings of Rathke's cleft cysts: significance of intracystic nodules. AJNR 2000;21:485–8.
(7) Castillo M, Smith J, Kwock L, Wilber K. Apparent diffusion coefficients in the evaluation of high-grade cerebral gliomas. AJNR 2001;22:60–4.
(8) Castillo M, Mukherji SK. Diffusion-weighted imaging in the evaluation of intracranial lesions. Semin Ultrasound CT MR 2000;21(6):405–16.
(9) Falini A, Calabrese G, Origgi D, Lipari S, Triulzi F, Losa M, et al. Proton magnetic resonance spectroscopy and intracranial tumours: clinical perspectives.. J Neurol 1996;243:706–14.
(10) Kozic D, Medic-Stojanoska M, Ostojic J, Ljubomir P, Nada V. Clinical applications of proton MR spectroscopy and treatment approaches in a patient with extrapituitary GH secreting macroadenoma. Neuro Endocrinol Lett 2007;28:560–4.
(11) Fan G, Sun B, Wu Z, Guo Q. Invivo single voxel proton MR spectroscopy in the differentiation of high grade gliomas and solitary metastasis. Clin Radiol 2004;59:77–85.
(12) Kwock L, Smith J, Castillo M, Ewend M, Cush S, Hensing T, et al. Clinical applications of proton MR spectroscopy in oncology. Technol Cancer Res Treat 2002;1:17–28.
(13) Chernov M, Hayashi M, Izawa M, Ono Y, Hori T. Proton magnetic resonance spectroscopy (MRS) of metastatic brain tumors: variations of metabolic profile. Int J Clin Oncol 2006;11:375–84.
(14) Chernov M, Ono Y, Muragaki Y, Kubo O, Nakamura R, Iseki H, et al. Differentiation of high-grade and low-grade gliomas using pattern analysis of long-echo single-voxel proton magnetic resonance spectroscopy (^{1}H-MRS). Neuroradiol J 2008;21:338–49.
(15) Dumrongpisutikul N, Wang Y, Zou L, Gao B. Distinguishing between germinomas and pineal cell tumors on MR imaging. AJNR 2012;33:550–5.
(16) Haughton V, Prost D, Rand S. Accuracy of single voxel proton MRS in distinguishing neoplastic from non-neoplastic brain lesions. Am J Neuroradiol 2003;18:1695–704.
(17) Mikhail F, Chernov, Takakazu K, Kosaku A, Yuko Ono, Suzek T, et al. Possible role of single-voxel ^{1}H-MRS in differential diagnosis of suprasellar tumors. J Neuroncol 2009;91:191–8.
(18) Majós C, Julià-Sapé M, Alonso J, Serrallonga M, Aguilera C, Acebes JJ, et al. Brain tumor classification by proton MR spectroscopy: comparison of diagnostic accuracy at short and long TE. AJNR 2004;25:1696–704.
(19) Pierallini A, Caramia F, Falcone C, Tinelli E, Paonessa A, Ciddio A, et al. Pituitary macroadenomas: preoperative evaluation of consistency with diffusion-weighted MR imaging – initial experience. Radiology 2006;239(1):223–31.
(20) Rogg JM, Tung GA, Andrson G, Cortez S. Pituitary apoplexy: early detection with diffusion-weighted MR imaging. Am J Neuroradiol 2002;23:1240–5.
(21) Sener RN, Proton MR. Spectroscopy of craniopharyngioma. Comput Med Imaging Graph 2001;25:417–22.
(22) Murakami R, Hirari T, Kitajima M, Fukuoka H, Toya R, Nakamura H, et al. MRI of pilocytic astrocytomas: usefulness of minimum ADC value for differentiation from high-grade gliomas. Acta Radiol 2008;49:462–7.
(23) Sumer Sethi. Spectroscopy in meningioma. AJNR Am J Neuroradiol May 1999;20:882–5.
(24) Okamoto K, Ito J, Ishkawa K, Sakai K, Tokigushi S. Diffusion-weighted echo-planner MR imaging in differential diagnosis of brain tumours and tumor-like conditions. Eur Radiol 2000;10:1342–50.
(25) Annette C, Douglas A, Jun Y, Zahirabbas M, Amr M, Eyas M. Diffusion-weighted imaging characteristics of primary CNS germinoma with histopathologic correlation: a retrospective study. Acad Radiol 2009;16(11):1356–65.